

Ionic conductivity and conduction mechanism studies on cellulose based solid polymer electrolytes doped with ammonium carbonate

M. I. H. Sohaimy¹ · M. I. N. Isa¹

Received: 26 March 2015 / Revised: 1 August 2016 / Accepted: 10 August 2016 /
Published online: 18 August 2016
© Springer-Verlag Berlin Heidelberg 2016

Abstract The present work deals with the formation of solid polymer electrolytes (SPE) from carboxy methylcellulose (CMC) and doped with ammonium carbonate ((NH₄)₂CO₃). The CMC–(NH₄)₂CO₃ SPE was characterized with electrical impedance spectroscopy (EIS) and transference number measurement (TNM) to understand its electrical and conduction mechanism. Fourier transform infrared (FTIR) were conducted to correlate the complexation of the SPE with conductivity and conduction mechanism. Complexation appears to occur mainly in CMC carboxyl group (C=O). The highest ionic conductivity obtained is $7.71 \times 10^{-6} \text{ Scm}^{-1}$ for samples incorporated with 7 wt% of (NH₄)₂CO₃. Lowest activation energy, E_a achieved is 0.21 eV corresponds to the highest conductivity sample. Ionic conductivity measurement at elevated temperature follows Arrhenius model. Dielectric study of the sample shows dependence to temperature, but not to the frequency. CMC–(NH₄)₂CO₃ SPE sample with the highest conductivity has transference number, t_+ of 0.98 proving of its conduction is predominantly cation. Quantum mechanical tunneling (QMT) was the best model to explain the conduction mechanism of the highest conductivity sample.

Keywords Modelling · Conductivity · Carboxy methylcellulose · Ammonium carbonate · Quantum mechanical tunneling

✉ M. I. N. Isa
ikmar_isa@umt.edu.my

M. I. H. Sohaimy
ibnuhyqal@gmail.com

¹ Advanced Materials Team, Ionic State Analysis (ISA) Laboratory, School of Fundamentals Science, Universiti Malaysia Terengganu, 21030 Kuala Terengganu, Terengganu, Malaysia

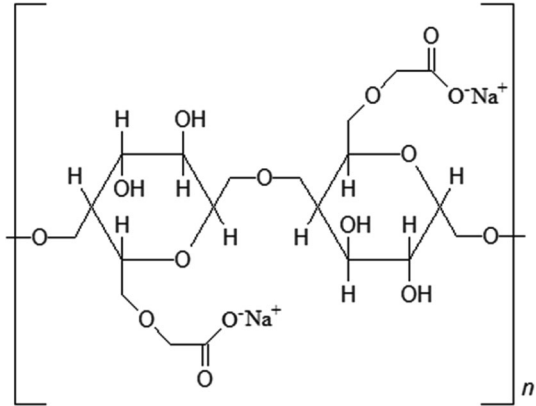
Introduction

Electrolytes are a chemical medium which transfer electrically charged ion between the anode and cathode through the charge–discharge process to conduct electricity [1]. For a long time, electrochemical devices were powered up using liquid electrolytes (LE) due to its high ionic conductivity. However, the problem persists with LE such as leakage, poor electrochemical stability and corrosion reactions with electrode [2]. The probability of electronic conduction also contributes to its drawbacks. These shortcomings of LE make it less suitable for electrochemical devices. New forms of electrolytes are needed to tackle the problems and subsequently become the new power sources for electrochemical devices [3].

Solid polymer electrolytes (SPE) have emerged as the best candidate to replace LE. Electrolyte in solid form behaves much like a liquid conductor [4]. The pioneering work on conducting polymer electrolytes was discovered by Wright in 1973 who use poly(ethylene) oxide (PEO) complexes with potassium thiocyanates and sodium iodide. There are several advantages SPE have that make it superior to LE such as good electrode–electrolyte contact, good mechanical properties, ease of handling, also improved safety hazards (no-leakage) [5, 6]. This discovery has spurred extensive studies in the field of material science and electrochemistry. Several types of conducting polymer electrolytes have been developed and investigated for, such as Polymethyl methacrylate (PMMA) [7], polyacrylonitrile (PAN) [8] and polyvinyl chloride (PVC) [9]. However, these types conducting polymer electrolytes are synthesized from synthetic materials derived from petroleum source which are facing exhaustion and this material is quite expensive [10].

Recently, natural or biodegradable materials have attracted much attention globally. The effects of global pollution and environment crises have forced consumers to demand safer, cheaper and environmentally friendly technology. Therefore, developments of SPE have turned its attention towards organic sources [11]. Organic material is normally regarded as an insulator, however, with certain tweaks to its structure, organic material can become semi-conductor material. Starch, Chitosan, cellulose and carrageenan are several organic sources have been developed as polymer electrolytes [12–14] carboxy methyl cellulose (CMC) a derivative of cellulose is an abundant natural product which has a white- to cream-coloured, tasteless, odourless and free-flowing powder [15, 16]. CMC (Fig. 1) is amphiphilic since it contains a hydrophobic polysaccharide backbone and many hydrophilic carboxyl groups ($-\text{CH}_2-\text{COONa}$). This characteristic allows for hydrogen bond to form easily. Due to its biodegradable properties and good film forming abilities, CMC is chosen as the polymer host [17, 18].

The aim of the present work is to develop a new SPE based on natural sources which is CMC as the host and doped with ammonium carbonate ($(\text{NH}_4)_2\text{CO}_3$) as the ionic dopant since ammonium salt is reported as a good proton sources for polymer system [19, 20]. The samples were prepared by solution casting technique and characterize for its complexation using Fourier transform Infrared (FTIR). The ionic conductivity, dielectric properties and AC conductivity were characterized using

Fig. 1 Chemical structure of CMC

electrical impedance spectroscopy (EIS) to understand the behaviour and the conduction mechanism of the electrolyte system while Transference number measurement (TNM) were used to confirm the conduction species of current systems.

Methodology

Sample preparation

2 g of CMC (acquired from Across Organics Co.) was stirred in distilled water until homogeneous. Different amount of $(\text{NH}_4)_2\text{CO}_3$ acquired from Sigma Aldrich (see Table 1) was then added into the CMC solution. The mixture solution was then stirred continuously until $(\text{NH}_4)_2\text{CO}_3$ is completely dissolved. Then, the CMC– $(\text{NH}_4)_2\text{CO}_3$ mixture was cast into petri dishes for drying process at room temperature (303 K). Final dried film was put inside a desiccator to further eliminate water presence in the film for another week. The CMC– $(\text{NH}_4)_2\text{CO}_3$ film was cut into suitable sizes for characterization.

Table 1 The CMC– $(\text{NH}_4)_2\text{CO}_3$ composition with its ionic conductivity, activation energy and regression values

Sample	CMC (g)	$(\text{NH}_4)_2\text{CO}_3$ (g)	Thickness (cm)	Ionic conductivity, σ (Scm^{-1})	Activation energy, E_a (eV)	Regression value, R^2
0 wt%	2	0.00	0.017	9.33E–09	0.23	0.99
1 wt%	2	0.02	0.011	1.89E–07	0.27	0.99
3 wt%	2	0.06	0.010	1.42E–06	0.24	0.94
5 wt%	2	0.11	0.012	1.79E–06	0.22	0.97
7 wt%	2	0.15	0.014	7.71E–06	0.21	0.94
9 wt%	2	0.20	0.013	3.51E–06	0.24	0.94
11 wt%	2	0.25	0.011	2.28E–06	0.31	0.94

Fourier transform infrared spectroscopy (FTIR)

Thermo Nicolet 380 Fourier Transform Infrared (FTIR) spectroscopies equipped with an attenuated total reflection (ATR) accessory with germanium crystal were used for complexation study. The sample was placed on germanium crystal and infrared light was passed through the sample within the frequency ranging from 4000 to 675 cm^{-1} at spectral resolution of 4 cm^{-1} . The data were then processed by a computer to form the spectrum bands.

Electrical impedance spectroscopy (EIS)

The electrical impedance spectroscopy (EIS) HIOKI 3532-50 LCR Hi-Tester interfaced to a computer with a frequency of 50 Hz–1 MHz was used to investigate the ionic conductivity of SPE films. The films were cut into a suitable size and placed between the stainless steel blocking electrodes of the sample holder. The software controlling the LCR tester calculates the real and imaginary impedance and plot a graph of negative imaginary impedance ($-Z_i$) versus real impedance (Z_r) to determine the bulk resistance (R_b) value which can be found from the intersection of the plot at real impedance axis for conductivity calculation. The equation for conductivity, σ is given by:

$$\sigma = \frac{t}{R_b A} \quad (1)$$

where t is the film thickness and A is the contact area of electrode-electrolytes. Dielectric constant ϵ_r is defined as

$$\epsilon_r(\omega) = \frac{Z_i}{\omega C_o (Z_r^2 + Z_i^2)} \quad (2)$$

where $C_o = \epsilon_o A/t$ (ϵ_o is permittivity of free space), $\omega = 2\pi f$ (f is frequency), z_i is imaginary impedance and z_r is real impedance.

Jonscher's Power Law (UPL) can be used to analyze the AC conductivity phenomenon [21].

$$\sigma(\omega) = \sigma_{dc} + A\omega^s \quad (3)$$

$$\sigma_{ac} = A\omega^s \quad (4)$$

where $\sigma(\omega)$ is the sum of AC and DC conductivity where σ_{dc} is frequency independent component. A is temperature dependent parameter and s is the power law exponent with a range from $0 < s < 1$. And the AC conductivity can be obtained from dielectric loss, ϵ_i at every frequency [22].

$$\sigma_{ac} = \epsilon_o \epsilon_i \omega \quad (5)$$

Taking Eqs. 4 and 5 and applied logarithm rule, it gives

$$\ln \varepsilon_i = \frac{\ln A}{\varepsilon_o + (S - 1) \ln \omega} \tag{6}$$

where:

$$\varepsilon_i(\omega) = \frac{Z_r}{\omega C_o(Z_r^2 + Z_i^2)} \tag{7}$$

Transference number measurement (TNM)

To confirm the type of ionic species in the SPE system, transference number measurements were done to correlate the diffusion phenomenon to the conductivity behaviour of the SPE system. Current polarization techniques were employed to measure the ionic transference number using the circuit built as shown in Fig. 2. A fixed DC 1.5 V was supplied into the circuit and the current values were monitored as a function of time. The equation below was used to calculate ionic transference, t_+ value:

$$t_+ = \frac{I_{\text{cation}}}{I_o} \tag{8}$$

$$I_{\text{cation}} = I_o - I_{ss} \tag{9}$$

where I_o = initial current, I_{ss} = steady-state current.

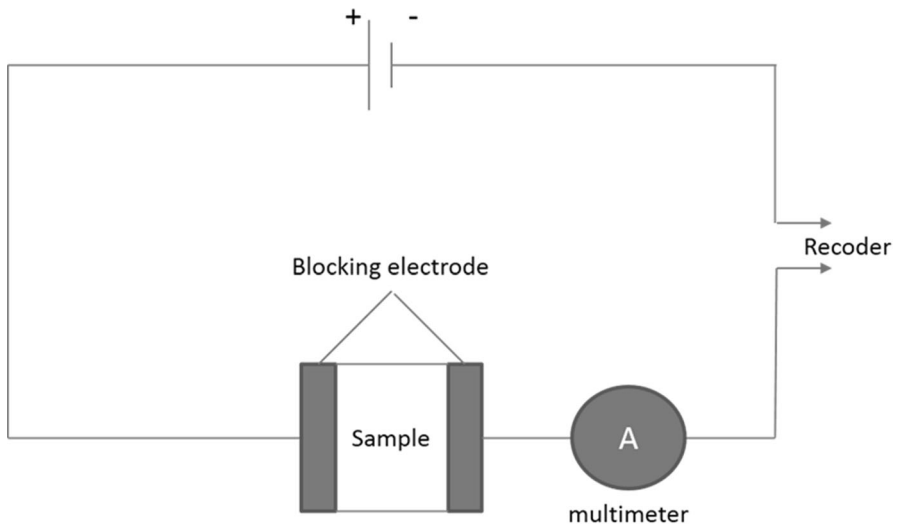


Fig. 2 Transference measurement circuit

Results and discussion

Complexation analysis

Complexation between the host (CMC) and ionic dopant ($(\text{NH}_4)_2\text{CO}_3$) in the CMC– $(\text{NH}_4)_2\text{CO}_3$ SPE system was conformed using an IR spectrometer. The complexation can be correlated to the IR spectra changes such as band shifting, the emergence or disappearance of the IR spectrum band. Figure 3 shows the spectral band for CMC– $(\text{NH}_4)_2\text{CO}_3$ SPE in the range of 1200–1800 cm^{-1} . From previous work done by Samsudin and Kamarudin, the complexation between ammonium salts and CMC took place in band range of 1040–1600 cm^{-1} [10, 23]. In the present work, several spectra band peaks can be seen in those ranges. The peak at 1591 cm^{-1} comes from C=O of carboxyl (COO^-) stretching of CMC [10, 20, 23]. The peak at 1417 and 1322 cm^{-1} belong to the C–H₂ scissoring and O–H bending, respectively [24, 25].

From Fig. 3, addition of $(\text{NH}_4)_2\text{CO}_3$ lead to some changes in the IR spectrum band. The C=O peak appears to weaken as more $(\text{NH}_4)_2\text{CO}_3$ were added into the system suggesting that complexation has occurred. New hump also appears at 1635 cm^{-1} when added with 7 wt% of $(\text{NH}_4)_2\text{CO}_3$. Further increase of $(\text{NH}_4)_2\text{CO}_3$

Fig. 3 FTIR spectra of CMC– $(\text{NH}_4)_2\text{CO}_3$ SPE at wavenumber 1200–1800 cm^{-1}

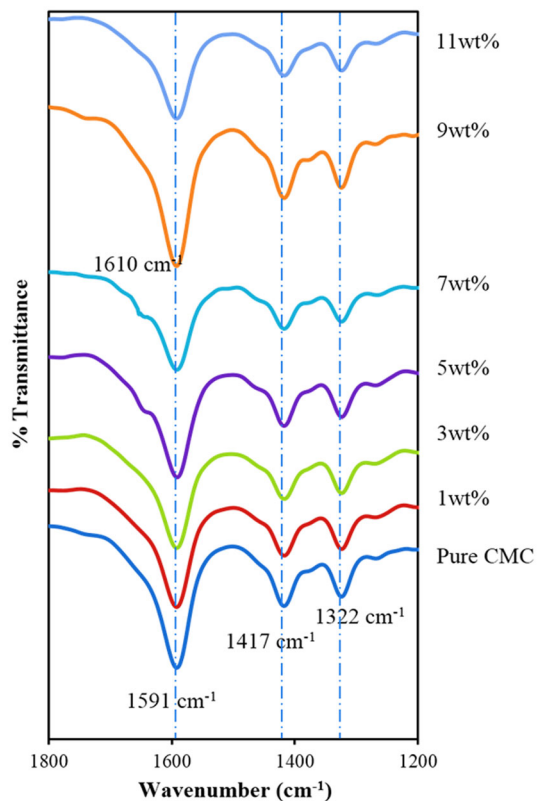
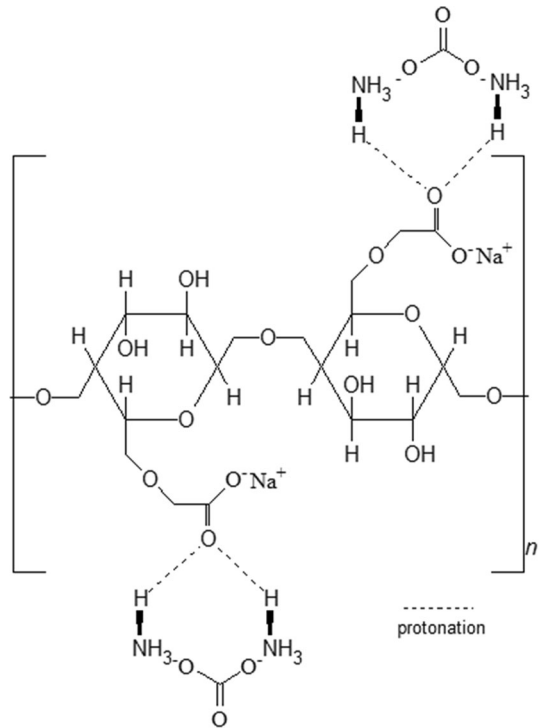


Fig. 4 Interaction between $(\text{NH}_4)_2\text{CO}_3$ with CMC through NH_4 group



shows that the humps disappear probably due to ions aggregation. It is believed that the complexation occurs at $\text{C}=\text{O}$ peak are due to the presence of lone pair electron which would attract free ions. The new peak observed are associated to H^+ originating from $(\text{NH}_4)_2\text{CO}_3$ [23]. The conduction species in polymer-ammonium salt system are due to proton (H^+) from the ammonium groups as proven by Hema et al. and Samsudin et al. [10, 26]. The migration of H^+ is apparent because in ammonium ions (NH_4^+), all hydrogen atoms are bound differently where one will be strongly bonded and another one loosely bonded while the rest are identically bonded. The loosely bound H^+ can dissociate with ease and move from one site to another. Two ammonium groups are present in ammonium carbonate salts thus it is suggested that either ammonium group will provide the proton needed. The proposed movement of protons is shown in Fig. 4.

Conductivity analysis

The ionic conductivity of $\text{CMC}-(\text{NH}_4)_2\text{CO}_3$ SPE system at ambient temperature is tabulated in Table 1. It can be observed that the ionic conductivity value increases with addition of ionic dopant. The value increase from $9.33 \times 10^{-9} \text{ Scm}^{-1}$ for pure CMC samples (0 wt% $(\text{NH}_4)_2\text{CO}_3$) to optimum ionic conductivity value of $7.71 \times 10^{-6} \text{ Scm}^{-1}$ for samples incorporated with 7 wt% of $(\text{NH}_4)_2\text{CO}_3$. This demonstrated that $(\text{NH}_4)_2\text{CO}_3$ has integrated well into the SPE system to provide

conducting species which in this case protons (H^+), therefore, resulting in increased of conductivity. From literature [16, 20, 23], CMC based SPE is amorphous in nature. Thus, it is expected that the current system is also amorphous. The amorphous nature will lower the energy barrier for ion movement compared to crystalline solid. The amorphous nature coupled with low bonding strength (H-bonding) allow H^+ to move easily when subjected to electric field. Beyond 7 wt%, the ionic conductivity of CMC– $(NH_4)_2CO_3$ SPE system dropped rapidly. This observed behaviour is believed due to the ions re-associate back forming neutral aggregates [27]. Additionally the dipole interaction between protons in the SPE increases at higher ionic dopant concentration which in turn reduces ionic mobility and thus the conductivity [28] (Table 1).

The ionic conductivity behaviour for CMC– $(NH_4)_2CO_3$ SPE system at elevated temperature (303–333 K) is shown in Fig. 5. Temperature study was carried out to analyze the ionic conduction mechanism of the natural SPE system. The plot shows that the ionic conductivity of all samples increased with increasing temperature confirming Arrhenius behaviour where regression values close to unity ($R^2 \approx 1$). The increased conductivity can be related to free-volume theory and segmental motion of the polymer [29, 30]. The polymer chain will vibrate in small segments as it receives energy from heat. This, in turn, creates bigger free volume enough for mobile protons to migrate through inter-chain and intra-chain movements hence the increased conductivity. This behaviour at elevated temperature is almost similar to ionic crystals [31]. The temperature relation with conductivity can be related by the following Arrhenius equation,

$$\sigma = \sigma_o \exp(E_a/kT) \quad (10)$$

where σ_o is the pre-exponential factor, E_a is the activation energy, k is the Boltzmann constant and T is the absolute temperature [in Kelvin (K)]. The E_a is calculated from a linear fit of the temperature dependence plot and listed in Table 1. It is

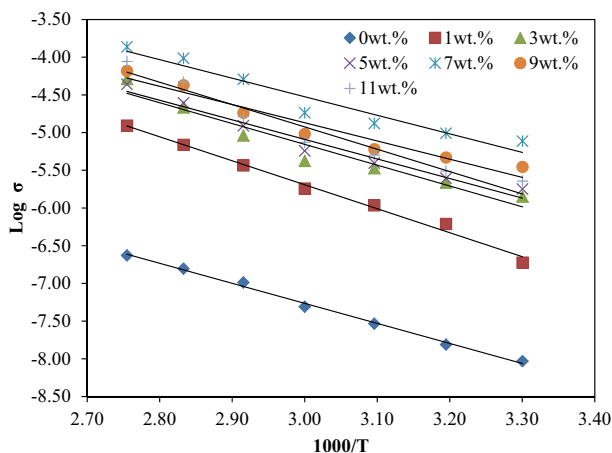


Fig. 5 The ionic conductivity behaviour of CMC– $(NH_4)_2CO_3$ SPE system at elevated temperature

noted that for the CMC–(NH₄)₂CO₃ SPE system, the sample with the highest ionic conductivity has the lowest activation energy, E_a (0.21 eV). Lower E_a indicates that the H⁺ will need less energy to be released from hydrogen bond that binds it at one coordinating site (C=O) to migrate to another coordinating site thus creating vacancies [19]. The vacancies created will then be filled by other H⁺. The ionic conduction process occurs from the whole process of vacancies forming and filling.

Figure 6 presented the (a) number of mobile ions η , (b) ionic mobility μ and (c) diffusion coefficient D of selected CMC–(NH₄)₂CO₃ SPE system at various temperatures. The value was calculated using Rice and Roth method [32]. The number of mobile ions, η increased as (NH₄)₂CO₃ content increases. This indicates that (NH₄)₂CO₃ has successfully dissociated creating more mobile ions during the doping process resulting in increase ionic conductivity. However, at higher (NH₄)₂CO₃ the conductivity decrease while η increases. This behaviour is believed due to the overcrowding of mobile ions which causes the pathway for ions migration to congest causing the mobility (μ) and diffusion coefficient (D) to decrease which in turn decrease the ionic conductivity value (see Fig. 6a–c). The number of mobile ions, η also increase with increasing temperature implies that ammonium salts dissociate more ions when heat are supplied resulting to increased ionic conductivity. The mobility (μ) and diffusion coefficient (D) also increase with temperature confirming that segmental motion and free-volume theory affected the ionic conductivity value.

Dielectric analysis

At low frequency region, the dielectric constant values of all samples (Fig. 7) are of the highest value indicating that electrode polarization and space charge effects have occurred [33]. In the low frequency region, the mobile ions are able to follow along the electric field direction before being trapped at the electrode–electrolyte interface to form hetero charge layers [34]. According to Majid and Arof [36], this implies that the mobile ions tend to accumulate at low frequencies giving it enough time for the charges to build up at the interface before the applied field changes direction, hence giving a higher value of ϵ_r .

At higher frequency region, the electric field orientation, acting on the medium occurs so fast that there is no time for ion diffusion throughout the medium following the direction of the electric field. As a result, the polarization due to the charge accumulation decreases and so does the ϵ_r values. Dielectric value would later drop and become saturated with increasing frequency as observed in Fig. 7 [34–37]. For sample 9 and 11 wt%, the dielectric value appears to decrease. The decreased in dielectric value are due to the decreased number of H⁺ from ions aggregation as mentioned in earlier sections. The ions aggregation also reduces the mobility of ions by blocking the migration pathway. Khiar et al. stated that the ϵ_r increases at higher temperatures are due to the higher charge carrier density [33].

The dielectric constant value of the sample with the highest conductivity at elevated temperature is shown in Fig. 8. From the figure, the ϵ_r value increased with increasing temperature. As temperature rises, the degree of salt dissociation and re-dissociation of ion aggregates increases resulting in the increase number of free ions

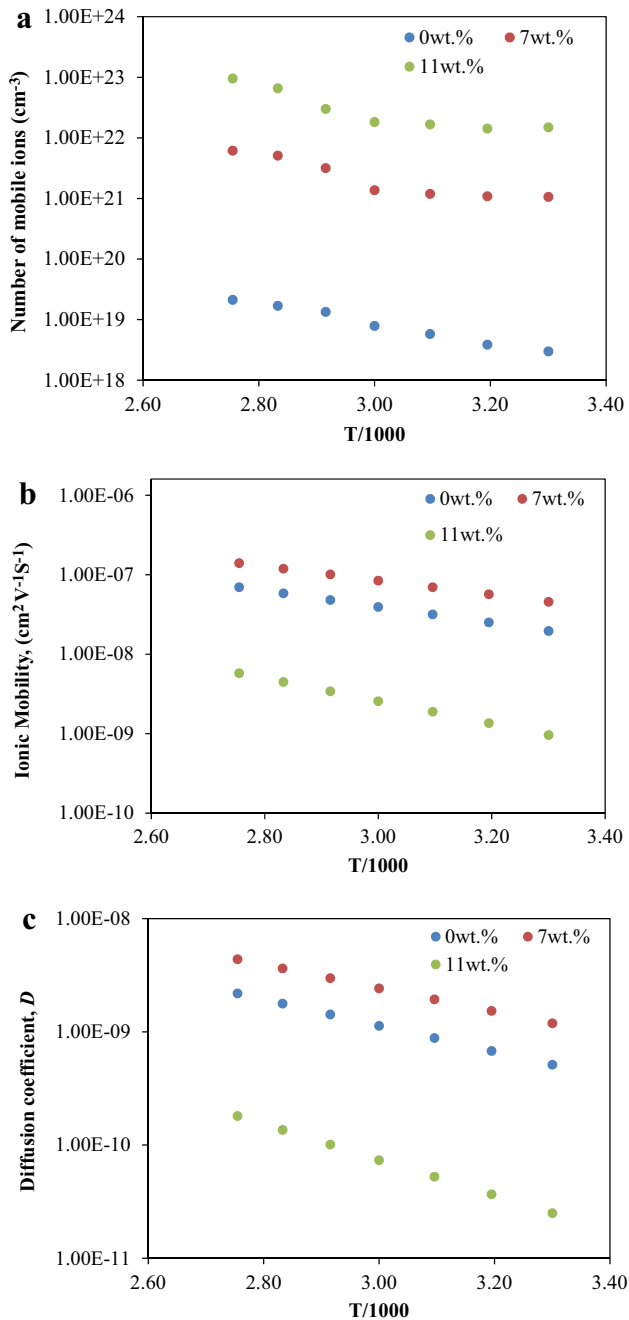


Fig. 6 Transport properties of CMC-(NH_4) $_2$ CO $_3$ SPE system: **a** number of mobile ions, **b** ionic mobility and **c** diffusion coefficient

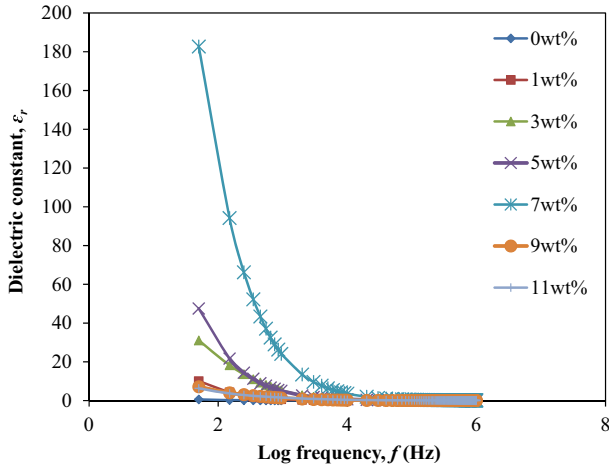


Fig. 7 Dielectric constant values for CMC–(NH₄)₂CO₃ SPE system with frequency at varying composition

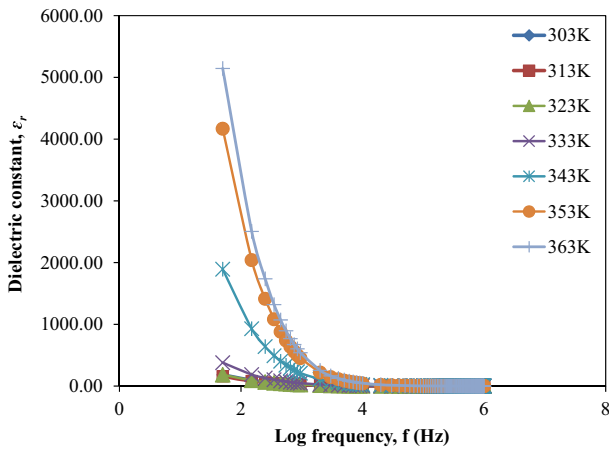


Fig. 8 Dielectric constant values at elevated temperature for CMC–(NH₄)₂CO₃ SPE system sample added with 7 wt% of (NH₄)₂CO₃

or charge carrier density and thus the dielectric value. The free volume, area inside the SPE as discussed before also contributed to the increased ϵ_r value.

Transference number analysis

The transference number was conducted to determine the contribution of conduction species of an electrolyte system (cationic, anionic or electronic) to the overall ionic conductivity. If an electrolyte system is to be applied in a battery system, the ionic transference number, t_+ need to be higher along with its ionic conductivity. This is because, low transference number, t_+ value will lead to an increase in concentration

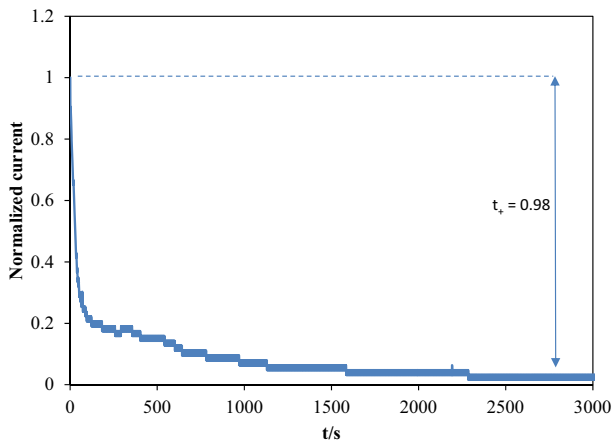


Fig. 9 Normalized current versus time plot for CMC-(NH₄)₂CO₃ with the highest conductivity

Table 2 Comparison of transference number of current work with another system

Electrolyte system	Transference number, t_+	References
PVA-PVdF-NH ₄ SCN	0.96	Muthuvinayagam and Gopinathan [40]
PVA-NH ₄ Br	0.96	Hema et al. [24]
PEO-LiBorate	0.79	Tao et al. [36]
MC-NH ₄ F	0.69	Aziz et al. [26]
CMC-OA	0.76	Chai and Isa [41]
CMC-(NH ₄) ₂ CO ₃	0.98	Present work

gradient of ions and decrease of working current. Thus, this will eventually lead to battery failure [38, 39]. The plot of the normalized current against time is shown in Fig. 9. The initial total current decreases with time and achieved a steady state current. At steady state, the ionic species are depleted (polarization). On the other hand, the residue current flows are due to electronic movement of the electrolytes. The transference numbers of 0.98 were achieved for the highest conductivity sample. This proved that the conduction species are primarily cation. Table 2 summarizes the transference value with other electrolyte systems. The table indicates that the transference number obtained from current works is higher compared to other system.

Conduction modelling analysis

Universal Jonscher power laws (UPL) were used for conduction modelling analysis as mention in the methodology section. Figure 10 shows the frequency dependence of dielectric loss, ϵ_i at elevated temperature of the sample with the highest conductivity. The value of exponent S can be obtained from the slope at higher

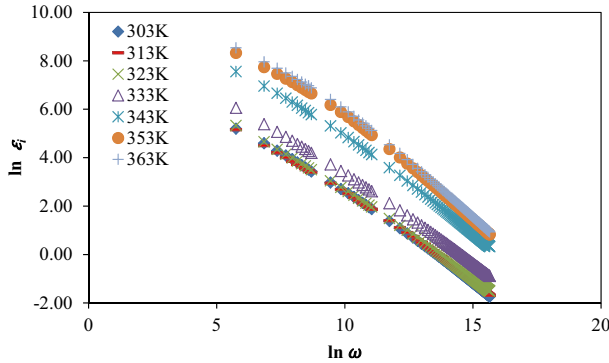


Fig. 10 The plot of $\ln \epsilon_i$ vs $\ln \omega$ for sample added with 7 wt% of $(\text{NH}_4)_2\text{CO}_3$

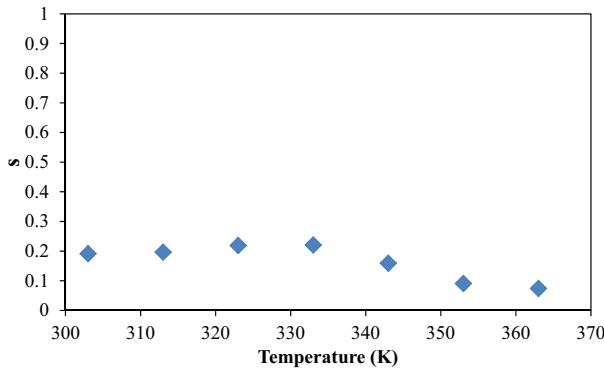


Fig. 11 Exponent S values for CMC– $(\text{NH}_4)_2\text{CO}_3$ for the highest conductivity sample

frequency where, according to [19, 20] there is no or minimal space charge polarization. The value of S with temperature was plotted in Fig. 5.

To find out how the conduction mechanisms in the system behave, one can suggest the appropriate AC conduction model based on the behaviour of value exponent S whether it is independent of temperature (QMT) [42] increase with temperature (SPH) [19], decrease with temperature (CBH) [43] or is it both temperature and frequency dependent (OLPT) [44]. From Fig. 11, there are little or no changes to the S values and can be said to behave in QMT conduction mechanism model. For QMT model, in this model, the polarons (in this case is made up of the protons and their stress fields) are able to tunnel through the potential barrier with the addition of $(\text{NH}_4)_2\text{CO}_3$ in the system that exists between two possible complexation sites [45]. Shukur et al. [46] stated that the ionic hopping between two sites not only occurs by jumping over a barrier, but can also accompany by QMT.

Conclusion

The SPE system constructs from CMC and doped with $(\text{NH}_4)_2\text{CO}_3$ has been successfully prepared via solution cast techniques. The optimum conductivity for CMC– $(\text{NH}_4)_2\text{CO}_3$ system is $7.71 \times 10^{-6} \text{ Scm}^{-1}$. The temperature dependence of the system appears to obey Arrhenius behaviour. The highest conductivity has the lowest activation energy, E_a implying it needs lower energy for ions migrations. Conduction process is governed not entirely by η , but also μ and D . From dielectric studies, ϵ_r shows to increase with each addition of $(\text{NH}_4)_2\text{CO}_3$ composition into the SPE system. The ϵ_r was found to increase at elevated temperature, but decreases at higher frequency. The conduction species have been confirmed from H^+ as proved in TNM analysis. The conduction behaviour of the system doped with 7 wt% of $(\text{NH}_4)_2\text{CO}_3$ is found to tunnel through the potential barrier following the quantum mechanical tunneling (QMT) model where the S value is independent of temperature. Present work shows a promising performance to be applied in an electrochemical application such as battery, fuel cell or super-capacitor. Although further improvement of the system is needed to increase the ionic conductivity as current ionic conductivity value is still low.

Acknowledgments The authors would like to thank Ministry of Education (MOE) for financial aid through ERGS (55101) and PRGS (54245) grant scheme. The school of Fundamental Science, Universiti Malaysia Terengganu for all their technical and research support for this work to be successfully completed. Special thanks to Advanced Materials Team (AMT) group members for proofreading this manuscript.

References

1. Saikia D, Chen-Yang YW, Chen YT, Li YK, Lin SI (2008) Investigation of ionic conductivity of com-posite gel polymer electrolyte membranes based on P(VDF-HFP), LiClO₄ and silica aerogel for lithium ion battery. *Desalination* 234:24–32
2. Kim HJ, Boysen DA, Newhouse JM, Spatocco BL, Chung B, Burke PJ, Bradwell DJ, Jiang K, Tomaszowska AA, Wang K, Wei WF, Ortiz LA, Barriga SA, Poizeau SM, Sadoway DR (2013) Liquid metal batteries: past, present, and future. *Chem Rev* 113:2075–2099
3. Goriparti S, Miele E, Angelis FD, Fabrizio ED, Zaccaria RP, Capiglia C (2014) Review on recent progress of nanostructured anode materials for Li-ion batteries. *J Power Sources* 257:421–443
4. Armand M (1994) The history of polymer electrolytes. *Solid State Ionics* 69:309–319
5. Geiculescu OE, Yang J, Blau H, Bailey-Walsh R, Creager SE, Pennington WT, DesMarteau DD (2002) Solid polymer electrolytes from dilithium salts based on new bis [(perfluoroalkyl) sulfonyl] diimide di anions. Preparation and electrical characterization. *Solid State Ionic* 48:173–183
6. Amrtha B, Hariharan K (2007) Ionic transport studies on (PEO) 6:NaPO₃ polymer electrolyte plasticized with PEG₄₀₀. *Eur Polymer J* 43:4253–4270
7. Bohnke O, Frand G, Rezrazi M, Rousselot C, Truche C (1993) Fast ion transport in new lithium electrolytes gelled with PMMA. 1. Influence of polymer concentration. *Solid State Ionics* 66:97–104
8. Voigt N, Wüllen LV (2012) The mechanism of ionic transport in PAN-based solid polymer electrolytes. *Solid State Ionics* 208:8–16
9. Ramesh S, Ng KY (2009) Characterization of polymer electrolytes based on high molecular weight PVC and Li₂SO₄. *Curr Appl Phys* 9(2):329–332
10. Samsudin AS, Lai HM, Isa MIN (2014) Biopolymer materials based carboxymethyl cellulose as a proton conducting biopolymer electrolyte for application in rechargeable proton battery. *Electrochim Acta* 129:1–13

11. Ramesh S, Chiam WL, Arof AK (2011) Ion conducting corn starch biopolymer electrolytes doped with ionic liquid 1-butyl-3-methylimidazolium hexafluorophosphate. *J Non-Cryst Solids* 357:3654–3660
12. Kumar M, Tiwari T, Srivastava N (2012) Electrical transport behaviour of bio-polymer electrolyte system: potato starch + ammonium iodide. *Carbohydr Polym* 88(1):54–60
13. Du JF, Bai Y, Pan DA, Chu WY, Qiao LJ (2009) Characteristics of proton conducting polymer electrolyte based on chitosan acetate complexed with $\text{CH}_3\text{COONH}_4$. *J Polym Sci Part B Polym Phys* 47(6):549–554
14. Cabello SDP, Mollá S, Ochoa NA, Marchese J, Giménez E, Compañ V (2014) New bio-polymeric membranes composed of alginate-carrageenan to be applied as polymer electrolyte membranes for DMFC. *J Power Sources* 265:345–355
15. Adinugraha MP, Marseno DW (2005) Haryadi Synthesis and characterization of sodium carboxymethyl cellulose from Cavendish banana pseudo stem (*Musa cavendishii* LAMBERT). *Carbohydr Polym* 62:164–169
16. Chai MN, Isa MIN (2013) The Oleic Acid Composition Effect on the Carboxymethyl Cellulose Based Biopolymer Electrolyte. *J Crystallization Process Technol* 3:1–4
17. Heydarzadeh HD, Najafpour GD, Nazari-Moghaddam AA (2009) Catalyst-free conversion of alkali cellulose to fine carboxymethyl cellulose at mild conditions. *World Appl Sci J* 6(4):564–569
18. Sassoa C, Beneventia D, Zeno E, Conil MP, Chaussia D, Belgacema MN (2011) Carboxymethyl cellulose: a conductivity enhancer and film-forming agent for processable polypyrrole from aqueous medium. *Synth Met* 161:397–403
19. Buraidah MH, Teo LP, Majid SR, Arof AK (2009) Ionic conductivity by correlated barrier hopping in NH_4I doped chitosan solid electrolyte. *Phys B* 404:1373–1379
20. Samsudin AS, Khairul WM, Isa MIN (2012) Characterization on the potential of carboxy methylcellulose for application as proton conducting biopolymer electrolytes. *J Non-Cryst Solids* 358(8):1104–1112
21. Raghu S, Kilarkaje S, Sanjeev G, Nagaraja GK, Devendrappa H (2014) Effect of electron beam irradiation on polymer electrolytes: change in morphology, crystallinity, dielectric constant and AC conductivity with dose. *Radiat Phys Chem* 98:124–131
22. Samsudin AS, Isa MIN (2012) Structural and ionic transport study on CMC doped NH_4Br : a new types of biopolymer electrolytes. *J Appl Sci* 12(2):174–179
23. Kamarudin KH, Isa MIN (2013) Structural and DC ionic conductivity studies of carboxy methylcellulose doped with ammonium nitrate as solid polymer electrolytes. *Int J Phys Sci* 8(31):1581–1587
24. Biswal DR, Singh RP (2004) Characterisation of Carboxymethyl Cellulose and Polycrylamide graft copolymer. *Carbohydr Polym* 57:379–387
25. Tongdeesootorn W, Mauer LJ, Wongruong S, Sriburi P, Rachtanapun P (2011) Effect of carboxymethyl cellulose concentration on physical properties of biodegradable cassava starch-based film. *Chem Cent J* 5(6):1–8
26. Hema M, Selvasekerapandian S, Sakunthala A, Arunkumar D, Nithya H (2008) Structural, vibrational and electrical characterization of PVA– NH_4Br polymer electrolyte system. *Physica B* 403(17):2740–2747
27. Samsudin AS, Isa MIN (2011) New types of biopolymer electrolytes: ionic conductivity study on CMC doped with NH_4Br . *J Curr Eng Res* 1:7–11
28. Nik Aziz NA, Idris NK, Isa MIN (2010) Proton conducting polymer electrolytes of methylcellulose doped ammonium fluoride: conductivity and ionic transport studies. *International Journal of the Physical Sciences* 5(6):748–752
29. Macedo PB, Litovitz TA (1965) On the relative roles of free volume and activation energy in the viscosity of liquids. *J Chem Phys* 42:245
30. Cohen MH, Grest GS (1982) Erratum: liquid-glass transition, a free-volume approach. *Phys Rev B* 26:6313
31. Samsudin AS, Isa MIN (2012) Characterization of carboxy methylcellulose doped with DTAB as new types of biopolymer electrolytes. *Bull Mat Sci* 35(7):1123–1131
32. Idris NK, Nik Aziz NA, Zambri MSM, Zakaria NA, Isa MIN (2009) Ionic conductivity studies of chitosan-based polymer electrolytes doped with adipic acid. *Ionics* 15:643–646
33. Khair ASA, Puteh R, Arof AK (2006) Conductivity studies of a chitosan-based polymer electrolyte. *Phys B* 373:23–27
34. Woo HJ, Majid SR, Arof AK (2013) Effect of ethylene carbonate on proton conducting polymer electrolyte based on poly(ϵ -caprolactone) (PCL). *Solid State Ionics* 252:102–108

35. Ganea CP (2012) New approach of the ac electrode polarization during the measurements of impedance spectra. *Rom J Phys* 57:664–675
36. Majid SR, Arof AK (2005) Proton-conducting polymer electrolyte films based on chitosan acetate complexed with NH_4NO_3 salt. *Physica B* 355(1–4):78–82
37. Saroj AL, Singh RK (2012) Thermal, dielectric and conductivity studies on PVA/Ionic liquid [EMIM][EtSO₄] based polymer electrolytes. *J Phys Chem Solids* 73:162–168
38. Tao R, Zhao Y, Fujinami T (2007) Lithium borate–PEO polymer electrolytes characterized with high lithium ion transference numbers. *Mater Sci Eng B* 137(1–3):69–73
39. Lu N, Yu MH, Chi WF, Fu MW, Jyh TL (2007) A simple method for synthesizing polymeric lithium salts exhibiting relatively high cationic transference number in solid polymer electrolytes. *Solid State Ionics* 178(5–6):347–353
40. Muthuvinayagam M, Gopinathan C (2015) Characterization of proton conducting polymer blend electrolytes based on PVdF-PVA. *Polymer* 68:122–130
41. Chai MN, Isa MIN (2013) Electrical characterization and ionic transport properties of carboxyl methylcellulose-oleic acid solid polymer electrolytes. *Int J Polym Anal Charact* 18:280–286
42. Hafiza MN, Isa MIN (2014) Ionic conductivity and conduction mechanism studies of cmc/chitosan biopolymer blend electrolytes. *Res J Recent Sci* 3(11):50–56
43. Nasri S, Megdiche M, Gargouri M (2014) Electrical conduction and dielectric properties of a newly synthesized single phase: $\text{Ag}_{0.4}\text{Na}_{0.6}\text{FeP}_2\text{O}_7$. *Phys B* 451:120–127
44. Farag AAM, Fadel M, Yahia IS (2012) Analysis of the electrical properties of p–n GaAs homo-junction under dc and ac fields. *Curr Appl Phys* 12:1436–1444
45. Isa MIN, Samsudin AS (2013) Ionic conduction behavior of cmc based green polymer electrolytes. *Adv Mater Res* 802:194–198
46. Shukur MF, Ibrahim FM, Ithnin Majid NA, Kadir MFZ (2013) Electrical analysis of amorphous cornstarch-based polymer electrolyte membranes doped with LiI. *Phys Scr* 88:1–9